

A Time Correlated Single Photon Counting Setup for High Temporal Resolution Measurements of the Temporal Response of Organic Scintillators

Jacob Sebastian¹, Bethany Goldblum^{1,2}, Josh Brown¹, and Thibault Laplace¹

¹University of California, Berkeley

²Lawrence Berkeley National Laboratory

April 2023

Abstract

A Time Correlated Single Photon Counting (TCSPC) system was developed to measure the energy-dependent temporal response of organic scintillators to neutron and γ -ray irradiation. This novel rendition of the canonical TCSPC setup was designed to minimize the primary contributors to the temporal uncertainty in a TCSPC measurement. Three factors were identified as major contributors to the temporal uncertainty of the system: the temporal resolution of the single photon counter, the ability of the system to determine the beginning of any given scintillation pulse, and uncertainties arising from the geometry of the scintillators. Efforts to minimize these sources of uncertainty will be discussed.

1 Introduction

When radiation is incident on a scintillator it transfers energy to the base by ionizing or exciting electrons. The heavier the particle, the greater this ionization and excitation density is, and the greater the density of ionization and excitation the greater the effect of ionization quenching. This ionization quenching leads to differences in pulse shape based off the mass and energy of the incident radiation. However, this phenomenon is not well represented in commonly available models of scintillation pulse shape of organic scintillators [1].

Several models exist that look to describe the scintillation pulse shape of organic scintillators [2] [3] [4] [5]. However, each model fails to accurately reflect pulse shapes under certain conditions. For instance, the Birks model fails to describe proton light yield over a broad energy range, and the Voltz et al. model of scintillation fails to account for the delayed scintillation component's dependency on ionization density [1]. Thus these commonly used specific luminescence models are not empirically reflecting the scintillation process in organic scintillators. There does not exist a reliable physics-based scintillation model in the literature [6]. In order to push forward modeling of organic scintillator response, energy dependent, high temporal resolution measurements of the scintillator pulse shape are necessary.

The precise measurement of scintillators timing properties are needed to provide a better understanding of the scintillation mechanism. For applications, it is required to calculate the best

coincidence time resolution achievable by a given material [7], or can be a needed input to image reconstruction algorithms in single volume detectors [8]. Most organic scintillators have rise times estimated to be faster than 1 ns and decay times on the order of nanoseconds to tens of nanoseconds. In order to capture the temporal response of faster scintillators for which the rise time of the PMT is slower or of the same order of magnitude as our quantity of interest, direct coupling to a PMT is insufficient. A new method must be employed, Time correlated single photon counting (TCSPC) allows the temporal response of fast scintillators to be captured with high resolution.

The temporal response of fast organic scintillators is lacking from the literature and where rise and decay times are available they are often cited without reference to uncertainty nor collection method. This lack inhibits the use of these fast organic scintillators in applications where an accurate temporal response would be a fundamental input for modeling of the system or likelihood reconstruction, such as applications in arms control, nonproliferation, medical imaging, and meta-materials development.

This paper will review efforts to modernize the canonical TCSPC example from Bollinger and Thomas [9], the characterization of the temporal uncertainty of this modernized TCSPC setup, and conclude with some thoughts on future work and potential applications.

2 Experimental Setup

TCSPC methods can be used to reconstruct the temporal response of scintillators with high temporal resolution. The basic theory behind TCSPC methods is that the shape of the scintillation pulse can be reconstructed by taking the time difference between the excitation of the scintillator and the emission of a single photon from that scintillation event.

In the example from Bollinger and Thomas [9], a closely coupled PMT is used to determine the time corresponding to the beginning of the scintillation event. A loosely coupled PMT provides a stop signal, receiving an average of less than 0.5 photons per scintillation event. The probability of that single photon occurring at a given time during the scintillation event is proportional to the intensity of the light output at that time. The setup captures less than one single photon at the stop detector per scintillation pulse, to take advantage of this probability as well as to enhance the dynamic range of the system by several order of magnitude.

Therefore by taking the difference between the beginning of a scintillation event, and the observation of a single photon at the stop detector over the course of several hundred thousand events, a reconstruction of the scintillator pulse shape can be created with high temporal resolution. A diagram of Bollinger and Thomas’s TCSPC setup is provided in Figure 1.

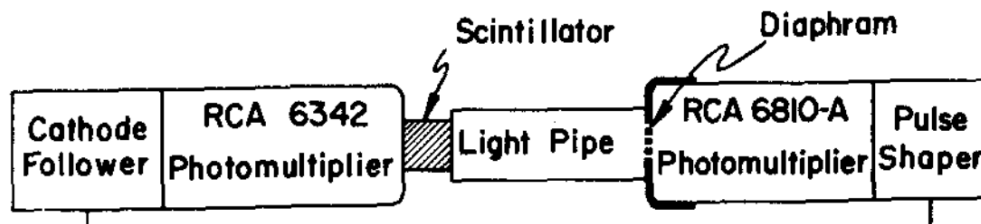


Figure 1: Diagram of Bollinger and Thomas’s TCSPC setup [9].

Improvements to the Bollinger and Thomas setup were implemented to allow for higher fidelity measurements. The scintillator is closely coupled to two modern PMTs (Hamamatsu H-6533) with low transit time spread to reduce the uncertainty on the start time of the scintillation event.

Two PMTs were employed to observe the start time of the scintillation event because the time difference between the two signals can be used to determine the uncertainty in the setups ability to determine the start time, as well as because it reduces the uncertainty in observing the start time by a factor of two. This is explained in more detail in Section 3.2.

A Photonis MCP-PMT PP-2365-AD with sub-15 ps temporal uncertainty was used as the single photon counter. Loose coupling between the scintillator was achieved using a standoff distance. The metric used to establish that the single photon counter was in the single photon range was that no more than one in every one hundred primary events results in a single photon count at the single photon counter. The system was read out using a LeCroy WaveSurfer oscilloscope with a sampling rate of 10 GHz, triggering on coincidences between the primary PMTs and the single photon counter. A diagram of the TCSPC setup constructed at Lawrence Berkeley Labs is provided in Figure 2.

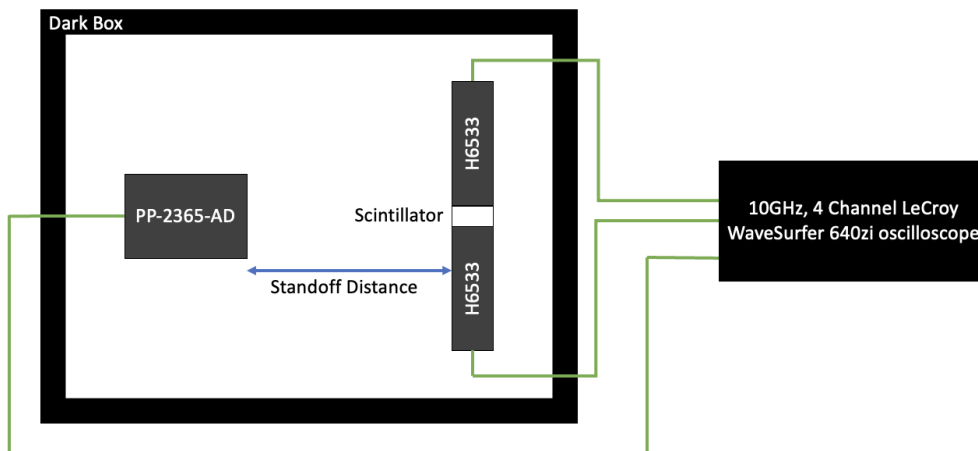


Figure 2: Diagram of Updated TCSPC Setup.

3 Temporal Uncertainty

To reconstruct the temporal response using the TCSPC method, the time between the start of the scintillation event, t_p , and emission of the single photon, t_e , must be measured. This quantity is referred to as the coincidence time, C_t , and is represented by:

$$C_t = t_e - t_p \quad (1)$$

In order to obtain the start time of the scintillation event, t_p , the 50% pick-off times of two closely coupled PMTs, t_{p1} and t_{p2} , were averaged together. The temporal offsets, $t_{pos,1}$ and $t_{pos,2}$, then need to be applied to this observed quantity due to the transit time of the PMTs to fully reflect the start time of the scintillation event. Thus t_p is given by:

$$t_p = \frac{t_{p1} + t_{p2}}{2} - \frac{t_{pos,1} + t_{pos,2}}{2} \quad (2)$$

In order to obtain the time at which an observed single photon was emitted from the scintillator, the 50% pick-off time of the single photon counter was taken, t_{spc} . However, this observable is also subject to the transit time of the MCP-PMT and the time of flight of the single photon across the standoff distance. Thus, a temporal offset, t_{spcos} , needs to be applied to account for the transit

time of the MCP-PMT, as well as the time of flight of the photon $\frac{L}{c}$ in order to reflect the time of emission of the single photon from the scintillator. Thus, t_e can be given as:

$$t_e = t_{spc} - \frac{L}{c} - t_{spcos}, \quad (3)$$

where L is the photon path length, and c is the speed of light. Taking the difference between these measured quantities should result in a measurement of the coincidence time:

$$\begin{aligned} C_t &= t_e - t_p \\ C_t &= t_{spc} - \frac{L}{c} - t_{spcos} - \frac{t_{p1} + t_{p2}}{2} + \frac{t_{pos,1} + t_{pos,2}}{2} \\ &= t_{spc} - \frac{t_{p1} + t_{p2}}{2} - \left(\frac{L}{c} + t_{spcos} - \frac{t_{pos,1} + t_{pos,2}}{2} \right) \end{aligned} \quad (4)$$

The error in the determination of t_{spc} , t_{p1} , and t_{p2} is negligibly small. Additionally, because the two primary PMTs are the same model, it can be assumed that $\sigma_{pos,1} = \sigma_{pos,2}$. Thus, the temporal resolution of our system can be taken to be the uncertainties of the quantities in the parenthetical in the final line of equation 4:

$$\sigma_{sys} = \sqrt{\sigma_{pos,1,2}^2 + \sigma_{spcos}^2 + \frac{\sigma_L^2}{c^2}} \quad (5)$$

The measurement of these individual uncertainties are the subject of the remainder of this section.

3.1 Temporal Resolution of the Photon Counter, σ_{spcos}

The time at which a single photon is incident on our single photon counter, t_{spc} , corresponds to the 50% pickoff time of the MCP-PMT single photon signal. Thus, the uncertainty in t_{spc} is the temporal resolution of our single photon counter.

In a previous rendition of this system which used a PMT-210 as its single photon counter, this uncertainty was quantified by using a laser with precise timing and a set of neutral density filters to ensure only single photons were impinging on the single photon counter. By comparing the photon count time with the laser sync signal, a distribution of the time spread of the photon count signal could be found. A diagram of this experimental setup can be found in Figure 3 and Figure 4 shows the difference between the laser sync signal and photon count time.

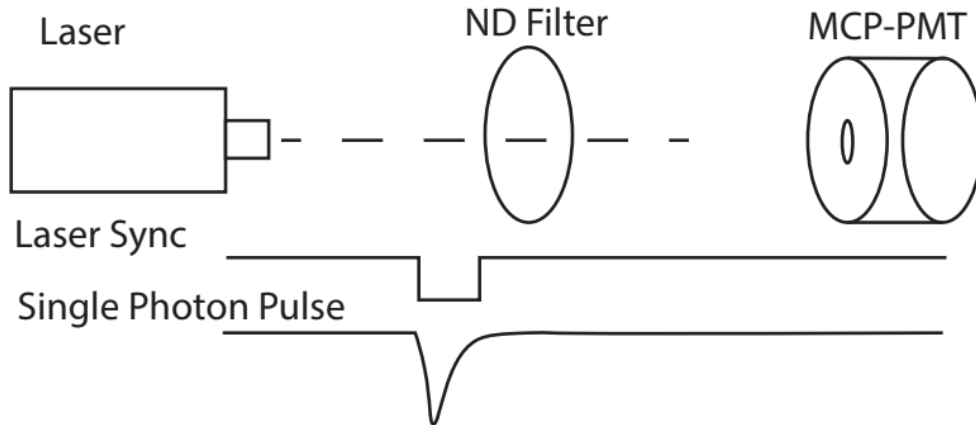


Figure 3: Diagram of experimental setup used to determine σ_{spcos}

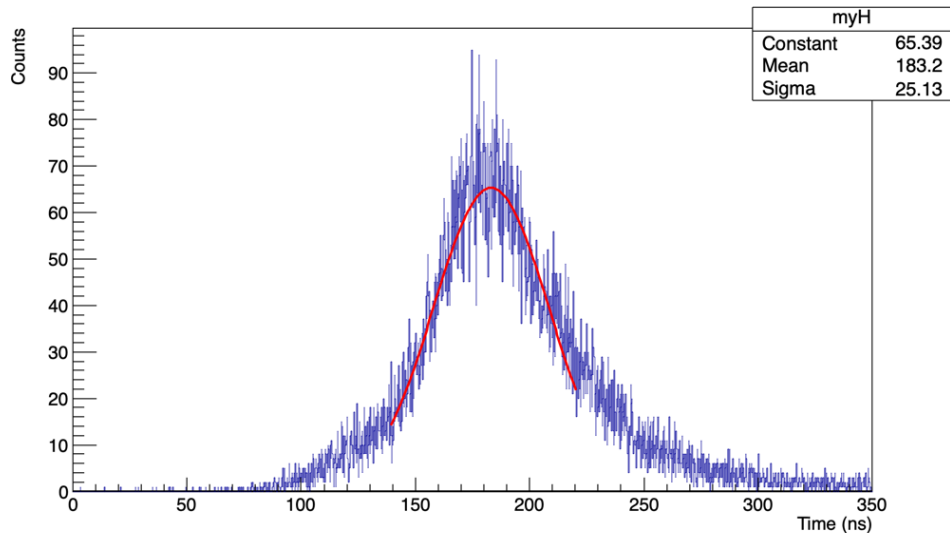


Figure 4: Histogram of the difference between the laser sync signal and single photon count time.

A Gaussian distribution was fitted to this peak and the sigma from that Gaussian was taken as the temporal resolution of the photon counter. While this distribution is clearly not perfectly Gaussian due to variant photoelectron pathlength in the microchannel plate [10], the Gaussian assumption is a good first order assumption and shows that the uncertainty of the single photon counter is on the order of 20 ps.

In the updated setup at Lawrence Berkeley Laboratory, a Photonis PP-2365-AD was used as the single photon detector with temporal uncertainty of 11 ps as reported by the manufacturer. So, the updated system is expected to have a smaller σ_{spcos} by a factor of at least two.

3.1.1 Coincidence Triggering and Cable Delays

As mentioned previously, the system triggers on coincidences between the primary PMTs and the single photon counter. In most TCSPC setups the primary PMT and the single photon counter PMT have similar transit times, meaning that triggering on coincidence is trivial. However, the MCP-PMT used as the single photon counter in this setup has a much faster transit time than the primary PMTs.

To assure that the setup can capture the relatively long decay tails of the temporal response, the primary signal needs to be observed before the single photon signal so that the oscilloscope can prime its trigger on the primary pulse and trigger on the single photon pulse.

A cable delay was introduced to insure that the signal from the MCP-PMT signal arrives after signals from the closely coupled PMTs. While this increased the temporal uncertainty of the single photon count time, it was determined that since the dominate uncertainty was still the uncertainty related to observing the start time of a scintillation pulse, this slight increase in uncertainty here was tolerable.

This also allows the setup to be run in two different modes. Without the cable delay, the setup can capture the rapid rise times of these temporal responses at the setups minimum temporal uncertainty. And with the cable delay, the setup can capture the relatively long decay tails with minimally reduced temporal resolution due to the increased jitter from the cable delay.

3.2 Uncertainty in determining, σ_{pos}

The start time of the scintillation event, t_p , is determined by taking the 50% pick-off time of both primary PMTs, t_{p1} and t_{p2} , averaging them together, and offsetting based off the transit times of the PMTs $t_{pos,1}$, and $t_{pos,2}$:

$$t_p = \frac{1}{2}(t_{p1} + t_{p2}) - \frac{t_{pos,1} + t_{pos,2}}{2}$$

Recall that the error in the determination of t_{p1} and t_{p2} is neglected because it is negligibly small and that $\sigma_{pos,1} = \sigma_{pos,2}$. Thus the uncertainty of t_p will be:

$$\sigma_{t_p}^2 = \sigma_{pos,1,2}^2 \quad (6)$$

In order to determine this uncertainty, the difference between the two primary signals is evaluated, Δt_{prim} . This quantity and its uncertainty is given by:

$$\Delta t_{prim} = t_{p1} - t_{p2} \quad \text{and} \quad \sigma_{\Delta t_{prim}}^2 = \sigma_{pos,1}^2 + \sigma_{pos,2}^2$$

It can be assumed that $\sigma_{pos,1} = \sigma_{pos,2}$, resulting in

$$\sigma_{\Delta t_{prim}}^2 = 2\sigma_{pos,1,2}^2$$

Returning to Equation 6 and substituting in $\frac{\sigma_{\Delta t_{prim}}^2}{2} = \sigma_{pos,1,2}^2$ it can be seen that:

$$\sigma_{t_p}^2 = \frac{1}{4}\sigma_{\Delta t_{prim}}^2$$

Thus the uncertainty of t_p can be taken as half of the uncertainty of Δt_{prim} . In order to determine the uncertainty of Δt_{prim} , the difference between 50% pick-off times for the two primary PMTs were plotted versus their pulse integral as represented in Figure 5. Then the uncertainty of the time difference as a function of pulse integral is plotted below the 2D histogram with the same x-axis.

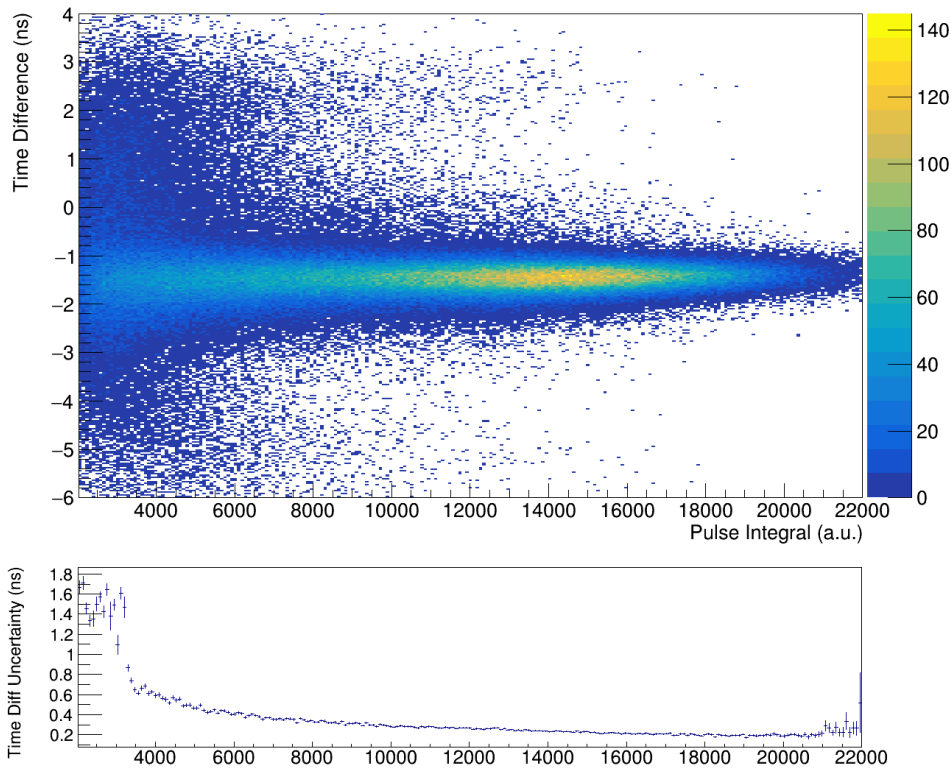


Figure 5: 2D Histogram of the difference between the primary signals versus their total pulse integral, and uncertainty of the time difference plotted versus pulse integral

As shown in Figure 5, the intensity of the pulse increases, the uncertainty of Δt_{prim} decreases. At this point in the system's characterization, a simple average over the energy range is taken in order to report an average temporal resolution of the system. It should also be noted that since the system's ability to observe a t_p is related to the speed at which a scintillator fluoresces, the uncertainty of t_p will change dependent on the scintillator being measured. Figure 5 was created using TCSPC data from the measurement of EJ-208. And so in this case, it can be reported that the system has a $\sigma_{pos}^- = 117$ ps when measuring EJ-208. Scintillators that produce more photons per unit time during the initial prompt fluorescence will result in smaller t_p uncertainty, so in the case of EJ-232Q, the t_p uncertainty is measured to be 45.9 ps.

Over the suite of scintillators measured in this setup, σ_{t_p} has consistently been the largest factor driving the systematic uncertainty of the system.

3.3 Photon path length variance, σ_L

The final identified influence on systematic uncertainty is the photon path length variance. Because scintillators have a refractive index that is 1.5, the path a photon takes to leave the scintillator and reach the single photon counter may increase the temporal uncertainty since a single photon that is generated during the initial rise of the temporal response will have a slightly different measured coincidence time depending on where in the scintillation volume the scintillation takes place.

In order to better understand how scintillator size effected photon path length variance a simplified model was created using Monte Carlo methods that sampled random points from a cylindrical

volume and then predicted flight times to a photon counter at some standoff distance, accounting for the increased refractive index of scintillators. This simplified model assumed that Snell’s law and internal reflection accounted for a small portion of the overall path length variance. Using this model the predicted temporal uncertainty due to photon path length variance is on the order of 15 ps. This uncertainty is much smaller than our dominant uncertainty σ_{prim} .

4 Future Work and Conclusions

Further characterization and analysis are required to fully validate and resolve the systematic uncertainty of the system. This includes a study of how photon path length variance impacts overall system uncertainty. This will be done by collected TCSPC data on scintillators of the same type, but of different sizes. The expected outcome of these measurements is to show that photon path length variance is of minimal concern for the scintillator size chosen for these measurements.

A suite of scintillators of varying sizes has been purchased and measurements will be taken with them. In order for the simplified model discussed in Section 3.3 to be validated, the overall systematic uncertainty should not change between scintillators of the same type but different sizes. And in order to validate the assumption that internal reflection accounts for a negligibly small portion of the overall photon path length variance, highly absorptive material has been purchased. This material will be applied to the scintillators to measure the impact of internal reflection on overall system uncertainty.

Once the system is validated and the system uncertainty is well characterized, the setup will be used to measure the temporal response of a suite of fast plastic scintillators in γ -ray fields.

The setup constructed at Lawrence Berkeley Lab was intentionally built in order to be able to take measurements in front of the 88-Inch Cyclotron at Lawrence Berkeley National Laboratory. A measurement campaign with a DT-breakup target at the 88-Inch Cyclotron will allow the system to measure energy dependent, neutron pure, pulse shapes. These neutron pure pulse shapes taken over a large energy range will allow us to explore what mechanisms are driving the scintillation process, and the impact of ionization density on pulse shape. The end goal of this work is to be able to construct more accurate, physics-based models of the temporal response of fast organic scintillators.

References

- [1] Thibault A Laplace et al. “Modeling ionization quenching in organic scintillators”. In: *Materials Advances* 3.14 (2022), pp. 5871–5881.
- [2] John Betteley Birks. *The theory and practice of scintillation counting: International series of monographs in electronics and instrumentation*. Vol. 27. Elsevier, 2013.
- [3] R Voltz et al. “Influence of the nature of ionizing particles on the specific luminescence of organic scintillators”. In: *The Journal of chemical physics* 45.9 (1966), pp. 3306–3311.
- [4] J Hong et al. “The scintillation efficiency of carbon and hydrogen recoils in an organic liquid scintillator for dark matter searches”. In: *Astroparticle Physics* 16.3 (2002), pp. 333–338.
- [5] CN Chou. “The nature of the saturation effect of fluorescent scintillators”. In: *Physical Review* 87.5 (1952), p. 904.
- [6] Juan J Manfredi et al. “The single-volume scatter camera”. In: *Hard X-Ray, Gamma-Ray, and Neutron Detector Physics XXII*. Vol. 11494. SPIE. 2020, pp. 121–131.

- [7] S. Gundacker et al. “Precise rise and decay time measurements of inorganic scintillators by means of X-ray and 511 keV excitation”. In: *Nuclear Instruments and Methods in Physics Research Section A: Accelerators, Spectrometers, Detectors and Associated Equipment* 891 (2018), pp. 42–52. ISSN: 0168-9002. DOI: <https://doi.org/10.1016/j.nima.2018.02.074>. URL: <https://www.sciencedirect.com/science/article/pii/S0168900218302286>.
- [8] Joshua Braverman et al. *Single-Volume Neutron Scatter Camera for High-Efficiency Neutron Imaging and Spectroscopy*. 2018. arXiv: 1802.05261 [physics.ins-det].
- [9] LM Bollinger and Ge E Thomas. “Measurement of the time dependence of scintillation intensity by a delayed-coincidence method”. In: *Review of Scientific Instruments* 32.9 (1961), pp. 1044–1050.
- [10] Ping Chen et al. “Photoelectron backscattering in the microchannel plate photomultiplier tube”. In: *Nuclear Instruments and Methods in Physics Research Section A: Accelerators, Spectrometers, Detectors and Associated Equipment* 912 (2018), pp. 112–114.